UC Irvine
UC Irvine Previously Published Works

Title

Dermal adipocytes protect against invasive Staphylococcus aureus skin infection

Permalink

https://escholarship.org/uc/item/8fq1r2p9

Journal

Science, 347(6217)

ISSN

0036-8075

Authors

Zhang, Ling-juan
Guerrero-Juarez, Christian F
Hata, Tissa
et al.

Publication Date

2015-01-02

DOI

10.1126/science.1260972

Peer reviewed

Dermal adipocytes protect against invasive *Staphylococcus aureus* skin infection

Ling-juan Zhang[1], **Christian F. Guerrero-Juarez**[2,3], **Tissa Hata**[1], **Sagar P. Bapat**[4], **Raul Ramos**[2,3], **Maksim V. Plikus**[2,3], and **Richard L. Gallo**[1,*]

[1]Division of Dermatology, University of California, San Diego (UCSD), La Jolla, CA 92093, USA

[2]Department of Developmental and Cell Biology, Sue and Bill Gross Stem Cell Research Center, University of California, Irvine, Irvine, CA 92697, USA

[3]Center for Complex Biological Systems, University of California, Irvine, Irvine, CA 92697, USA

[4]Nomis Foundation Laboratories for Immunobiology and Microbial Pathogenesis, The Salk Institute for Biological Studies, San Diego, La Jolla, CA 92037, USA

Abstract

Adipocytes have been suggested to be immunologically active, but their role in host defense is unclear. We observed rapid proliferation of preadipocytes and expansion of the dermal fat layer after infection of the skin by *Staphylococcus aureus*. Impaired adipogenesis resulted in increased infection as seen in *Zfp423^{nur12}* mice or in mice given inhibitors of peroxisome proliferator–activated receptor γ. This host defense function was mediated through the production of cathelicidin antimicrobial peptide from adipocytes because cathelicidin expression was decreased by inhibition of adipogenesis, and adipocytes from *Camp$^{-/-}$* mice lost the capacity to inhibit bacterial growth. Together, these findings show that the production of an antimicrobial peptide by adipocytes is an important element for protection against *S. aureus* infection of the skin.

Host defense against microbial infection involves the participation of several cell types. Owing to the rapid doubling time of many microbes, immediate protection provided by local resident cells—such as epithelial cells, mast cells, and resident leukocytes—is essential to restrict the spread of infection during the lag period before recruitment of additional cells, such as neutrophils and monocytes (1, 2). The production of antimicrobial peptides (AMPs) by local resident cells and recruited leukocytes is a key mechanism to limit pathogen growth (3-5).

Staphylococcus aureus is a major cause of skin and soft-tissue infections in humans, causing both local and systemic disease (6, 7). We observed that a large and previously

---

[*]Corresponding author. rgallo@ucsd.edu.

unrecognized expansion of the subcutaneous adipose layer was evident during the early response to *S. aureus* skin infection (Fig. 1A). The response to infection was confirmed with quantification of the abundance of adipocytes (Fig. 1B and fig. S1A), observations of an increase in lipid staining (fig. S1B), and increased activation of the adiponectin promoter as measured in *AdipoQcre;R26R* mice (Fig. 1C) (8). Adipocytes progressively increased in size after *S. aureus* infection (Fig. 1B), suggesting that the expansion of dermal adipose tissue occurs at least in part through hypertrophy of mature adipocytes. PREF1 and ZFP423 mark committed preadipocytes required for adipose tissue development and expansion (9-11). Proliferation of these preadipocytes at the site of infection was further confirmed with colocalization of PREF1 and ZFP423 with proliferation markers BrdU (Fig. 1D and fig. S1C) and Ki67 (fig. S1D). Additionally, dermal cells isolated from *S. aureus*–infected skin exhibited greater adipogenic potential than that of cells isolated from the same amount of uninfected skin, as indicated by lipid production and induction of adipocyte markers *Adipoq* and *Fabp4* in response to adipocyte differentiation medium (Fig. 1E and fig. S1E). Also supporting the conclusion that infection results in an increase of cells within the dermis with the potential to differentiate into adipocytes were observations of an increase of mRNA and protein for transcription factors driving preadipocyte differentiation, including *Cebpb*, *Pparg*, and *Cebpa* (Fig. 1F and fig. S1, D and F) (12, 13). Peroxisome proliferator-activated receptor-γ (PPARγ)-positive cells at the infected sites were negative for CD11b (fig. S1G), confirming that they were not myeloid cells. To test that cell proliferation was associated with adipocyte formation, we examined BrdU incorporation within the nuclei of adipocytes after multiple injections of BrdU (14) during the first 3 days after infection. A significant increase in the number of BrdU-positive nuclei was seen within cells from *S. aureus*–infected mice stained with the adipocyte surface protein Caveolin (Fig. 1G), thus confirming that adipocytes at the site of infection were at least partially derived from proliferative precursors. Together, these data showed that infection by *S. aureus* triggers preadipocyte proliferation and expansion of local dermal adipocytes.

We next tested whether adipocyte activation was essential for protection against *S. aureus* infection using *Zfp423* reporter mice and *Zfp423^nur12* mice in which adipogenesis is prominently impared (11, 15). Activation of Zfp423 during infection was confirmed by visualizing β-Gal staining on the underside of skin from infected *Zfp423^lacZ* reporter mice (Fig. 2A) (16). Immunostaining of infected *Zfp423^GFP* reporter mice (17) showed green fluorescent protein-positive (GFP⁺) cells localized within infected dermal adipose tissue and mostly colocalized with a fibroblast marker [platelet-derived growth factor receptor-α (PDGFRα)], but not with an endothelial cell marker (CD31) (Fig. 2B and fig. S2, A and B). After *S. aureus* infection, dermal adipose tissue in *Zfp423^nur12* mice expanded less than in control mice (fig. S2C). Immunostaining with the adipocyte marker Perilipin (PLIN) further confirmed that adipocyte formation was reduced in the *Zfp423^nur12* mice compared with control (fig. S2D). Impaired adipogenesis in *Zfp423^nur12* mice was accompanied by increased susceptibility to *S. aureus* skin infection at the site injected with bacteria (Fig. 2, C and D) and a subsequent systemic bacteremia that was not detectable in controls (Fig. 2E). Increased susceptibility to *S. aureus* in *Zfp423^nur12* mice was associated with decreased activation of PDGFRα⁺Sca1⁺ skin preadipocytes (fig. S2E) (18), but not with defective

leukocyte recruitment because there was no decrease in CD11b staining or neutrophil infiltration in the skin of *Zfp423^nur12* mice (fig. S2F).

To complement the observations made in *Zfp423^nur12* mice, we chemically inhibited adipogenesis by pretreating wild-type mice with bisphenol A diglycidyl ether (BADGE) or GW9662, both pharmacological inhibitors of PPARγ and acute chemical inhibitors of adipogenesis (14, 19, 20). Similarly to *Zfp423^nur12* mice, BADGE- or GW9662-treated mice showed decreased adipose expansion after *S. aureus* infection (fig. S3A) and became more susceptible to infection (Fig. 2, F to H, and fig. S3B). In BADGE-treated mice, PDGFRα⁺Sca1⁺ preadipocyte numbers appeared normal (fig. S3C), but PPARγ expression decreased (fig. S3D), suggesting as in a previous report (14) that inhibition of PPARγ impaired dermal adipose growth by blocking preadipocyte differentiation into adipocytes rather than by inhibiting the preadipocyte commitment process. Increased susceptibility to *S. aureus* in BADGE-treated mice was not caused by defective leukocyte recruitment (fig. S3E) nor by any impaired ability of blood neutrophils to kill *S. aureus* (fig. S3F). Because neutrophil function is a major factor in resisting *S. aureus* skin infection (6), this finding confirmed that the increased susceptibility to infection observed with PPARγ inhibitors was caused by their effect on adipocyte formation.

3T3-L1 cells are a well-characterized primary mouse preadipocyte line that can be induced to differentiate into mature adipocytes (21). To determine how adipocytes might protect against infection, a comparison of antimicrobial peptide (AMP) gene expression was done in 3T3-L1 undifferentiated preadipocytes (pAds) and differentiated adipocytes (Ads). This showed that mouse cathelicidin antimicrobial peptide (*Camp*) was strongly induced in Ads compared with pAds, whereas other AMPs belonging to the α- and β-defensin families did not show an increase in expression (Fig. 3A). *Camp* mRNA increased at day 1 after differentiation then decreased during later stages of differentiation (fig. S4A). *Camp* expression preceded expression of adipokines Resistin (*Retn*), Leptin (*Lep*), and *Fabp4*, whereas the relative expression of another AMP, *Defb14*, decreased during differentiation (fig. S4, B to H).

Cathelicidin protein peaked at day 2 to ~4 after differentiation and was abundantly detectable with Western blotting of cell extracts from differentiating pAds (fig. S4I). The size of cathelicidin detected by means of Western blot was consistent with the mCAP18 cathelicidin precursor protein (22). Cathelicidin was also found with Western blotting in adipocyte-conditioned medium (Fig. 3B). Secretion of cathelicidin protein preceded secretion of Resistin, Leptin, and FABP4 at days 2 to 4 after differentiation (Fig. 3B) and was similar to that of Collagen type-IV (COL4A1), which was produced 1 to 2 days after differentiation (23). Immunostaining of 3T3-L1 cells showed cathelicidin appearing simultaneously with lipid droplets in the cytoplasm of Ads (Fig. 3C) and localized in the early endosome, but not in the lysosome (fig. S4J).

To verify that cathelicidin was also produced by human adipocytes, we evaluated cultured primary human preadipocytes with reagents directed against human cathelicidin. The *CAMP* gene was strongly induced during differentiation (fig. S5A), and Western blot showed bands consistent with the cathelicidin precursor protein hCAP18 and a shorter peptide (fig. S5B).

This peptide appeared larger than LL-37, the mature peptide form of cathelicidin detected from human neutrophils (24), thus suggesting adipocytes may have an enzymatic processing system differing from that known in other cell types (25).

Cathelicidin mRNA was detected in the subcutaneous fat pad from 1- to ~2-week-old mice (fig. S6, A and B), a stage in which the tissue is undergoing early adipogenesis (26). *Camp* mRNA was more abundant in white adipose tissue than brown adipose tissue (fig. S6C). Cathelicidin protein immunostaining was detected in fat tissue from mice and humans (Fig. 3C) and was localized in the early endosome of adipocytes (fig. S6D). In a mouse model of diet-induced obesity, *Camp* mRNA measured with quantitative polymerase chain reaction (PCR) and cathelicidin protein levels estimated by means of Western blot (fig. S7, A and B) were more abundant in the subcutaneous fat pad from mice fed high-fat diet as compared with low-fat diet controls. High-fat diet increased both bone marrow adiposity and cathelicidin protein expression in bone marrow adipocytes (fig. S7C). Serum cathelicidin levels were also elevated in the high-fat diet group (Fig. 3D and fig. S7, D and E), similar to samples from overweight humans [body mass index (BMI) > 25] (Fig. 3E). The level of cathelicidin detected with enzyme-linked immunosorbent assay in serum (~50 ng/ml) was well below the amount of LL-37 necessary to inhibit *S. aureus* growth, which is typically above 2 to 5 mg/ml (27). Thus, the high local expression of cathelicidin is more likely to provide antimicrobial function than is the small increase in systemic cathelicidin found in obesity.

Cathelicidin mRNA production during 3T3-L1 differentiation was significantly enhanced when *S. aureus*-conditioned medium or ultraviolet (UV)–killed *S. aureus* was added to adipocyte differentiation medium (Fig. 3F), revealing that *S. aureus* directly enhances AMP production during adipocyte differentiation. Similar to 3T3-L1 cells, dermal cells isolated from *S. aureus*–infected skin, which were shown in Fig. 1E to exhibit high adipogenic potential, produced *Camp* mRNA and abundant cathelicidin protein preceding the production of FABP4 (Fig. 3G).

We next examined cathelicidin production during *S. aureus* infection by immunostaining infected mouse skin. Cathelicidin protein and mRNA were strongly induced in the fat layer at the site of infection (Fig. 4A and fig. S8A). Cathelicidin protein colocalized with expression of the adiponectin reporter β-Gal in AdipoQ-cre;R26R mice (fig. S8B) and COL4A1 (fig. S8, C and D), showing that cathelicidin was expressed in adipocytes in vivo during *S. aureus* infection, correlating with the increase in dermal adipocytes (Fig. 1) and its expression during early adipogenesis (Fig. 3B).

The precursor (~18 kD) and a peptide form (5 to ~10 kD) of cathelicidin were detected in differentiated 3T3-L1 adipocytes (Fig. 4B) and in the cell lysate of mouse adipose tissue (Fig. S9A). Similarly to cultured human adipocytes, the mouse adipocyte-derived cathelicidin peptide was slightly larger than mature cathelicidin-related antimicrobial peptide (CRAMP) derived from mouse neutrophils. We tested conditioned medium from differentiated 3T3-L1 adipocytes and observed that conditioned medium that contained secreted cathelicidin potently inhibited the growth of *S. aureus*, whereas conditioned medium from pAds that lacked cathelicidin did not (Fig. 4C). Brefeldin-A treatment blocked

cathelicidin secretion from adipocytes and abolished the antimicrobial activity of the conditioned medium derived from adipocytes (fig. S9B). Furthermore, extracts from wild-type mouse adipose tissue inhibited growth of *S. aureus* (Fig. 4D and fig. S9C) and *Pseudomonas aeruginosa* (Fig. S9D), but adipose tissue extracts from $Camp^{-/-}$ mice did not possess antimicrobial properties. $Camp^{-/-}$ mice did not differ from wild-type in their capacity to develop metabolic syndrome after 20 weeks of high-fat diet (fig. S10).

Mice in which adipose expansion was inhibited showed reduced defense against *S. aureus* infection, and this correlated with reduced cathelicidin. BADGE treatment of 3T3-L1 during differentiation inhibited *Pparg* and *Cebpa* mRNA and blocked *Camp* (fig. S11A). The expression of cathelicidin was less in mice treated with BADGE (fig. S11B) and in $Zfp423^{nur12}$ mice (Fig. 4, E and F), although the expression of cathelicidin seen in cells recruited to the site of infection was maintained. $Zfp423^{nur12}$ did not inhibit neutrophil recruitment as seen by a similar increase in abundance of the neutrophil marker (*Mpo*) after infection (fig. S11D). As expected, $Camp^{-/-}$ mice showed increased susceptibility to infection (3). However, $Camp^{-/-}$ mice treated with BADGE or GW9662 showed no further increase in infection (Fig. 4G and fig. S12), suggesting that the effects of BADGE on cathelicidin production from adipocytes was responsible for the increase in *S. aureus* infection in vivo.

These results show that a local increase in subcutaneous adipocytes is an important host defense response against skin infection. This observation is consistent with prior observations that adipocytes secrete a variety of bioactive adipokines and cytokines that mediate immune responses after injury (28) and now shows that adipocytes produce an AMP that can directly kill bacteria. Local expansion of dermal fat produces cathelicidin in response to infection, but this response appears to decline as adipocytes mature. The expansion of dermal fat in response to infection may also indirectly benefit immune defense by influencing other processes such as neutrophil oxidative burst, thus further amplifying the importance of the subcutaneous preadipocyte pool in preventing infections. Defective AMP production by mature adipocytes may explain observations of elevated susceptibility to infection during obesity and insulin resistance (29). Cathelicidin has also been shown to be proinflammatory (30). Therefore, the production of cathelicidin by adipocytes may also participate in the chronic, low-level inflammation observed in obesity (28).

Supplementary Material

Refer to Web version on PubMed Central for supplementary material.

ACKNOWLEDGMENTS

from R. Gupta under a material transfer agreement with Dana-Farber Cancer Institute. All the data reported in this manuscript are presented in the main paper and in the supplementary materials.

REFERENCES AND NOTES

1. Nestle FO, Di Meglio P, Qin JZ, Nickoloff BJ. Nat. Rev. Immunol. 2009; 9:679–691. [PubMed: 19763149]

2. Gallo RL, Hooper LV. Nat. Rev. Immunol. 2012; 12:503–516. [PubMed: 22728527]

3. Nizet V, et al. Nature. 2001; 414:454–457. [PubMed: 11719807]

4. Ong PY, et al. N. Engl. J. Med. 2002; 347:1151–1160. [PubMed: 12374875]

5. Pütsep K, Carlsson G, Boman HG, Andersson M. Lancet. 2002; 360:1144–1149. [PubMed: 12387964]

6. Miller LS, Cho JS. Nat. Rev. Immunol. 2011; 11:505–518. [PubMed: 21720387]

7. Musser JM, et al. Proc. Natl. Acad. Sci. U.S.A. 1990; 87:225–229. [PubMed: 1967495]

8. Eguchi J, et al. Cell Metab. 2011; 13:249–259. [PubMed: 21356515]

9. Sul HS. Mol. Endocrinol. 2009; 23:1717–1725. [PubMed: 19541743]

10. Hudak CS, et al. Cell Reports. 2014; 8:678–687. [PubMed: 25088414]

11. Gupta RK, et al. Nature. 2010; 464:619–623. [PubMed: 20200519]

12. Tanaka T, Yoshida N, Kishimoto T, Akira S. EMBO J. 1997; 16:7432–7443. [PubMed: 9405372]

13. Lefterova MI, et al. Genes Dev. 2008; 22:2941–2952. [PubMed: 18981473]

14. Festa E, et al. Cell. 2011; 146:761–771. [PubMed: 21884937]

15. Alcaraz WA, et al. Proc. Natl. Acad. Sci. U.S.A. 2006; 103:19424–19429. [PubMed: 17151198]

16. Cheng LE, Zhang J, Reed RR. Dev. Biol. 2007; 307:43–52. [PubMed: 17524391]

17. Gupta RK, et al. Cell Metab. 2012; 15:230–239. [PubMed: 22326224]

18. Driskell RR, et al. Nature. 2013; 504:277–281. [PubMed: 24336287]

19. Naveiras O, et al. Nature. 2009; 460:259–263. [PubMed: 19516257]

20. Schmidt BA, Horsley V. Development. 2013; 140:1517–1527. [PubMed: 23482487]

21. Green H, Kehinde O. Cell. 1975; 5:19–27. [PubMed: 165899]

22. Dorschner RA, et al. J. Invest. Dermatol. 2001; 117:91–97. [PubMed: 11442754]

23. Sillat T, et al. J. Cell. Mol. Med. 2012; 16:1485–1495. [PubMed: 21883898]

24. Sørensen OE, et al. Blood. 2001; 97:3951–3959. [PubMed: 11389039]

25. Sørensen OE, et al. J. Biol. Chem. 2003; 278:28540–28546. [PubMed: 12759353]

26. Kawaguchi N, et al. Am. J. Pathol. 2002; 160:1895–1903. [PubMed: 12000741]

27. Boman HG. J. Intern. Med. 2003; 254:197–215. [PubMed: 12930229]

28. Schäffler A, Schölmerich J. Trends Immunol. 2010; 31:228–235. [PubMed: 20434953]

29. Cawthorn WP, Scheller EL, MacDougald OA. J. Lipid Res. 2012; 53:227–246. [PubMed: 22140268]

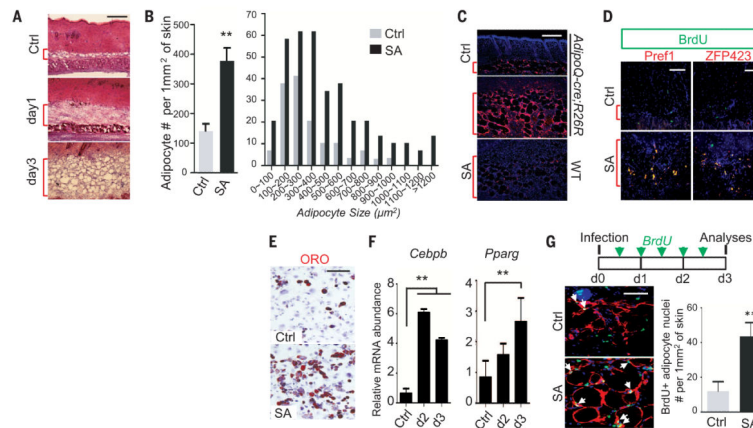30. Yamasaki K, et al. Nat. Med. 2007; 13:975–980. [PubMed: 17676051]

Fig. 1. Skin infection stimulates an increase in dermal adipocytes
(**A**) Hematoxylin and eosin staining of mouse skin injected with phosphate-buffered saline (PBS) control (Ctrl) or *S. aureus* (SA). Red brackets indicate subcutaneous adipose layer. Scale bars, 200 μm. (**B**) Quantification of the number and size distribution of Caveolin⁺/ Perilipin⁺ adipocytes 3 days after Ctrl or *S. aureus* injection (*n* = 3 to ~5 mice/group and 3 microscopy fields/mice). (**C**) Increase of adiponectin positive cells seen by staining for β-Gal (red) 3 days after *S. aureus* or Ctrl injection in *AdipoQcre;R26R* mice. Wild-type mice injected with *S. aureus* are shown as a staining control. Scale bars, 200 μm. Nuclei were stained with 4′,6-diamidino-2-phenylindole (DAPI) (blue). (**D**) Ctrl or *S. aureus*–infected mice (day 1) were injected with BrdU 4 hours before analysis. Proliferative preadipocytes were identified by means of yellow staining showing colocalization of PREF1 or ZFP423 (red) and BrdU (green). Scale bars, 100 μm. (**E**) Dermal cells were isolated from Ctrl or *S. aureus* (SA)–infected skin then treated with adipocyte differentiation medium for 5 days. Lipid production was shown by Oil-Red-O (ORO) staining. Scale bars, 200 μm. (**F**) Relative mRNA expression for *Cebpb* and *Pparg* (*n* = 3 mice/group) in skin after *S. aureus* infection. (**G**) (Top) Schematic of 3-day BrdU labeling experiments during *S. aureus* infection. (Left) Representative images for caveolin (red) and BrdU (green) staining of skin sections. Arrows indicate Caveolin⁺BrdU⁺ adipocytes. Scale bars, 50 μm. (Right) Quantification of the number of Caveolin⁺BrdU⁺ adipocytes (*n* = 3~5 mice/group and 3 microscopy fields/mice). All error bars indicate mean ± SEM; ** $P < 0.01$ (*t* test).
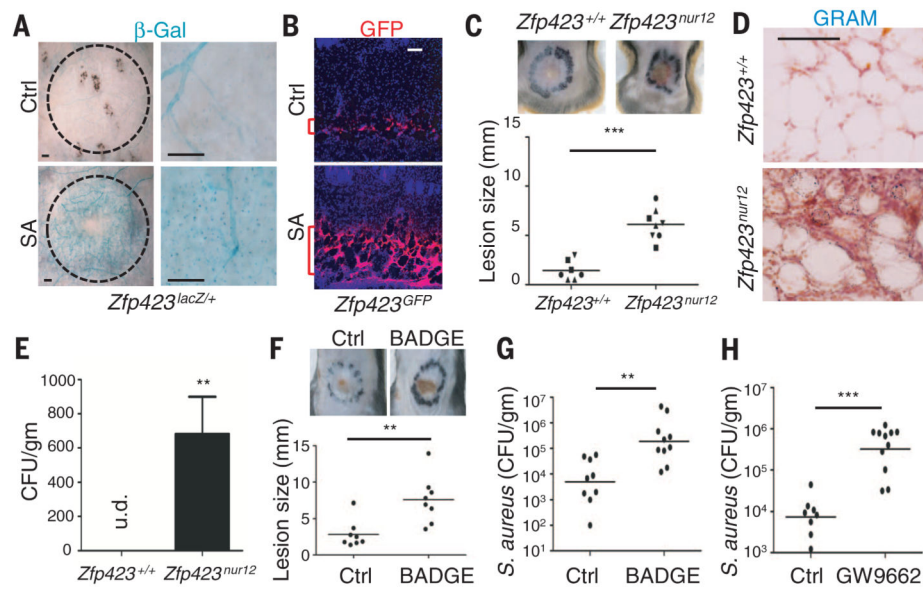
Fig. 2. Adipocytes are essential for host defense against *S. aureus* infection

(**A**) β-gal staining of the underside of *Zfp423^{lacZ/+}* skin 3 days after injection with PBS (Ctrl) or *S. aureus*. Injected area is indicated by dotted line. Scale bars, 1mm (left), 200 μm (right). (**B**) GFP immunostaining (red) of skin sections from Ctrl or *S. aureus*–injected *Zfp423^{GFP}* mice. Scale bars, 100 μm. (**C**) Infected lesion size in *Zfp423^{nur12}* or *Zfp423^{+/+}* mice (*n* = 7~8/group) and (**D**) bacteria in adipose observed by Gram staining (dark blue). Scale bars, 100 μm. (**E**) Systemic bacteremia detected 3 days after *S. aureus* skin injection in spleens isolated from *Zfp423^{nur12}* mice but not *Zfp423^{+/+}* mice (*n* = 3 mice/group). Scale bars, 200 μm. (**F** to **H**) BADGE or GW9662 increased susceptibility to *S. aureus* as observed by (**F**) increased lesion size and [(G) and (H)] increased *S. aureus* (CFU) from the skin calculated with plate counting (*n* = 8 to ~10/group). All error bars indicate mean ± SEM. ** *P* < 0.01, *** *P* < 0.001 (*t* test).
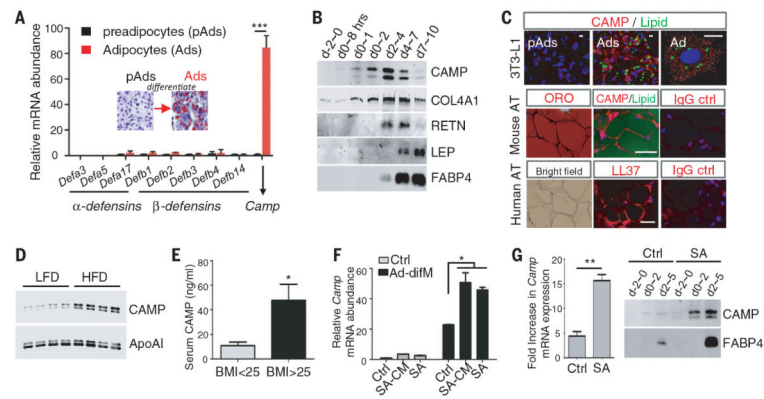
Fig. 3. Adipocytes produce cathelicidin antimicrobial peptide

(**A**) 3T3-L1 preadipocytes (pAds) were differentiated to adipocytes (Ads). Expression of mRNA for α-defensins, β-defensins, and cathelicidin (*Camp*) is shown (*n* = 3 cultures/group). (Inset) Oil-Red-O staining. (**B**) Western-blotting of conditioned media from differentiating 3T3-L1 cells. (**C**) Staining of 3T3-L1 cells or mouse and human subcutaneous adipose tissue (AT) by using lipid dye (Bodipy; green), mouse CAMP (red), Oil-red-O, or the human cathelicidin peptide LL37 (red) as indicated. Nuclei are counterstained with DAPI. Scale bar, 5 μm (3T3-L1) or 50 μm (adipose tissue). (**D**) C57BL6 mice fed with low-fat diet (LFD) or high-fat diet (HFD) for 4 weeks, and mouse serum was collected for Western blotting analysis by using CAMP and ApoAI antibodies. (**E**) Human serum cathelicidin measured in overweight (/BMI >25) or normal-weight human subjects (*n* = 10 subjects/group). (**F**) Camp mRNA expression levels were examined by quantitative reverse transcription PCR (RT-PCR) in 3T3L1 preadipocytes treated with or without adipocyte differentiation (Ad-difM) medium and with *S. aureus*–conditioned medium (SA-CM) or UV-killed *S. aureus* (SA). (**G**) Primary cultures of dermal cells isolated from Ctrl or *S. aureus*–injected skin were treated with Ad-difM. Relative *Camp* mRNA fold induction at day 2 compared with undifferentiated control were examined by means of quatitative (RT-PCR) (left); CAMP and FABP4 protein were detected in conditioned medium by means of Western blot (right). All error bars indicate mean ± SEM; *$P < 0.05$, **$P < 0.01$, ***$P < 0.001$ (*t* test).
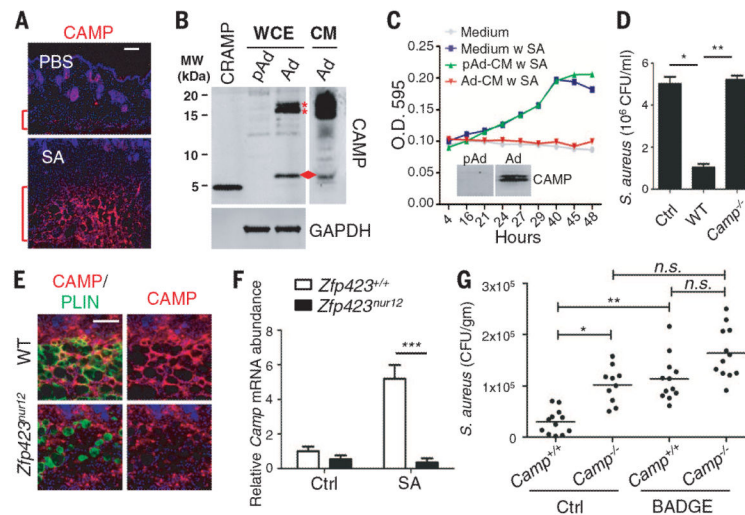
Fig. 4. Adipocytes kill bacteria by producing cathelicidin

(**A**) CAMP immunostaining (left) of adipose in mice infected with *S. aureus*. Scale bar, 100 μm. (**B**) Western-blotting of CAMP from whole-cell extracts (WCE) or conditioned medium (CM) from 3T3-L1 pAds or Ads. Red arrow indicates mature peptide form, and red asterisks indicate precursor forms of cathelicidin. Synthetic CRAMP peptide is shown as standard for the processed form of CAMP in neutrophils. (**C**) Growth curve of *S. aureus* in Ctrl medium or conditioned medium (CM) from pAd or Ad as indicated. (Inset) CAMP immunoblot in conditioned medium. (**D**) *S. aureus* growth in media alone (Ctrl) or with addition of protein extracted from subcutaneous adipose tissue from *Camp*^{+/+} or *Camp*^{−/−} mice ($n = 3$). (**E**) CAMP expression is suppressed in adipose in *Zfp423*-deficient mice. Scale bars, 100 μm. (**F**) Camp mRNA expression in *S. aureus*– or PBS-injected *Zfp423*^{+/+} and *Zfp423*[nur12] mice ($n = 5$ mice/group). (**G**) *Camp*^{+/+} or *Camp*^{−/−} mice were pretreated with BADGE or dimethyl sulfoxide (ctrl) before infecting with *S. aureus* and *S. aureus* survival in skin measured 3 days later ($n = 7$ to ~10 mice/group). All error bars indicate mean ± SEM. $*P < 0.05$, $**P < 0.01$, $***P < 0.001$ (one-way analysis of variance). Red brackets indicate subcutaneous adipose layer.